IEEE Access
Multidisciplinary ⋮ Rapid Review ⋮ Open Access Journal

Received September 13, 2020, accepted September 23, 2020, date of publication October 8, 2020,
date of current version November 6, 2020.

Digital Object Identifier 10.1109/ACCESS.2020.3029611

Research on Influence Factors and Acceleration Methods of Current Commutation

LIYAN ZHANG[1], (Graduate Student Member, IEEE), ENYUAN DONG[1], (Member, IEEE), RUIDA ZHUANG[2], YONGXING WANG[1], (Member, IEEE), YU ZHU[1], (Graduate Student Member, IEEE), AND JIYAN ZOU[1]

[1]School of Electrical Engineering, Dalian University of Technology, Dalian 116023, China
[2]State Grid Dalian Electric Power Supply Company Ltd., Dalian 116000, China

Corresponding author: Yongxing Wang (yxwang@dlut.edu.cn)

This work was supported in part by the National Natural Science Foundation of China under Grant 51877026.

ABSTRACT The vacuum interrupter is widely used due to the advantages of no arc-extinguishing medium and high insulation strength. However, the arc voltage generated by the commonly used CuCr contacts is low. In hybrid DC circuit breakers (DCCB), hybrid automatic transfer switches (ATS), medium voltage compound switches and other fields, it is difficult to rely on vacuum arc to complete natural commutation, which restricts the development of hybrid switches. In order to understand the current commutation process deeply, the influence of internal and external factors on the current commutation is analyzed by experiments. The coupling mathematical model of arc-commutated branch is established. The criterion for the success of current commutation is summarized. The parameters of the arc model are reconstructed through repeated breaking experiments to explore the influence of internal factors on the arc characteristics. Based on this, the influence law of arc current, contacts gap and transverse magnetic field (TMF) is analyzed. An acceleration method of current commutation is proposed. A prototype for accelerating experiments with an electromagnetic repulsion mechanism and TMF is developed. The commutated branch equivalent to practical applications is built. The experimental results show that the commutation time is effectively shortened and meets the requirements of practical applications through the acceleration method, which provides new thought for the development of hybrid switches.

INDEX TERMS Vacuum interrupter, current commutation, dynamic threshold current, TMF, average opening velocity, hybrid switches, parameters reconstruction.

I. INTRODUCTION

The action schemes of current-commutation type are more and more widely used due to the better current breaking capacity, more precise switching phase, lower steady-state loss and faster switching speed [1], [2]. In application fields such as hybrid ATS, hybrid DCCB, power electronic-mechanical hybrid phase-controlled switches and uninterruptible power supplies (UPS), the successful and rapid commutation of current is the key [3]–[5]. Therefore, it is of great significance for engineering to study the influence factors and acceleration methods of current commutation systematically.

In different applications, the current commutation process has been studied based on different topologies. The DCCB based on the combination of IGCTs and fast vacuum circuit breaker (VCB) has been carried out by Meyer at the EPFL (Ecole Polythectnique Federale de Lausanne) with the company Sécheron SA [6]. The fast switching of the hybrid automatic transfer switch (HATS) is realized in Huazhong University of Science and Technology [7]. But the fault current cannot be interrupted in this HATS. Tsinghua University has designed a fault current limiter based on vacuum arc current commutation at power frequency zero. The current commutation is analyzed with a commutated branch of reactor. The first peak of the fault current is not limited. The current commutation is realized only at power frequency zero. The commutating characteristics in 10kV natural-commutate hybrid DCCB are studied in [8]. The influence of contact material and circuit parameters on the commutation speed is analyzed. The arc voltage is increased by 3-5 V by changing the contact material. Tokyo Institute

The associate editor coordinating the review of this manuscript and approving it for publication was Xiaokang Yin.

of Technology investigates the effects of some parameters including the contact diameter, separation speed, and cable inductance in the SiC-MOSFET commutated branch on the threshold current of the arc-less commutation by using copper contacts [9]. The power electronic-mechanical hybrid phase-controlled switches are designed in [10]. The influence of the commutation speed on the opening window is analyzed. The theoretical model of current commutation based on vacuum arc is proposed in [11]. The two basic models of Zero Voltage Switch (ZVS) and Zero Current Switch (ZCS) of hybrid DCCB are summarized. However, there is no method to determine whether the commutation is successful or not. The internal factors affecting the dynamic characteristics of the arc are not analyzed.

In summary, the current commutation plays an important role in the power system. Vacuum interrupters are widely used in China's medium voltage power system [12], [13]. The voltage of the vacuum arc is low [14], [15]. The impedance of the medium voltage commutated branch is generally high. This restricts the development of hybrid switches and current limiters with commutated branches. Most of the previous researches are based on specific topology to study the current commutation process in related applications. Although the circuit model of current commutation has been established, the effect of influence factors has not been discussed in detail. There is a lack of analysis on whether the current commutation can be completed quickly and successfully. So far, there is no effective acceleration method of current commutation based on vacuum arc.

Thus, to analyze the law of influence factors and explore better acceleration methods, the current commutation is still needs to be further studied. This paper is organized as follows. In Section II, the influence law of internal and external factors in current commutation of vacuum arc is summarized. The criterion for the success of current commutation is proposed. In Section III, the effect of internal factors on the vacuum arc is deeply analyzed. We propose an acceleration method of current commutation based on this. In Section IV, the effectiveness of the acceleration method is successfully verified in the experiment. Finally, important conclusions are drawn based on the results of study in Section V.

II. INFLUENCE FACTORS

Regardless of the application and the topology of the circuit, current commutation can be simplified as an arc branch and a commutated branch in parallel. The natural-commutate process based on vacuum arc is shown in Fig. 1.

u_{arc} is the vacuum arc voltage. u_e is the threshold voltage when the power electronic devices are turned on. L is the inductive reactance of the commutated branch. R_{th1} is the equivalent resistance of the commutated branch. R_{th2} is the equivalent resistance of the arc branch. The loop equation can be expressed as

$$\begin{cases} u_{arc} + i_{arc}R_{th2} = u_e + L\dfrac{di_{pa}}{dt} + i_{pa}R_{th1} \\ i_s = i_{pa} + i_{arc} \end{cases} \quad (1)$$

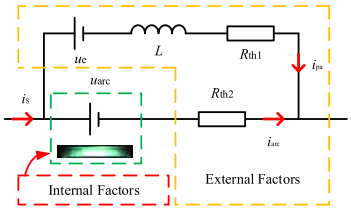

FIGURE 1. Topology of natural-commutate process. i_s is the current of the main loop. i_{arc} is the current of the arc branch. i_{pa} is the current of the commutated branch.

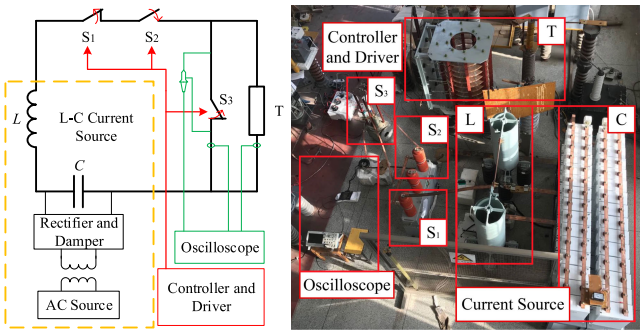

(a) Circuit topology (b) Test site

FIGURE 2. Test circuit topology and related equipment.

It can be seen that u_e, L, R_{th1}, u_{arc}, R_{th2} and i_s are the main factors affecting the commutation speed. They are divided into external factors and internal factors in this paper. The established factors for current limiting or breaking are called external factors, including the types of the commutated branches (resistive, inductive, power electronics), reactance value, initial phase and current amplitude of the main loop. The factors that affect the development of the arc are called internal factors, including the contact velocity, the arc current, and TMF. The influence factors and laws of the dynamic process of current commutation are fully experimentally analyzed, regardless of the specific topology of each application in this section. The test circuit and equipment are shown in Fig. 2.

The L-C oscillating current source is used as a high current generator. S_2 is an input switch. S_1 is an auxiliary switch. The contacts with axial magnetic field (AMF) are widely used in medium voltage VCBs. The arc voltage of the AMF contacts is low, which is bad for natural commutation. We will carry out research on this bad situation. Therefore, S_3 is a 10 kV VCB with cup-type AMF contacts. The total diameter of the contact is 55 ± 0.2 mm. The end diameter is 45 ± 0.2 mm. The vacuum interrupter diameter is 110 ± 1 mm. The opening distance is 10 mm. The interrupter of S_3 remains unchanged in this paper. When the test starts, S_2 is first put in, and a current with a frequency of 50 Hz is generated by the current source. Then S_3 opens and the current commutation starts. After the commutation, S_1 opens. The sequence of operations is shown in Fig. 3. The opening and closing of each switch are driven by charged capacitors through thyristors. T_1 and T_3 are the trigger signals of the thyristors for opening coils of S_1 and S_3. T_2 is the trigger signal for closing coil of S_2. When the

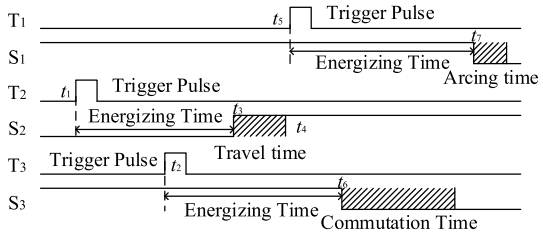

FIGURE 3. Action sequence of each switch.

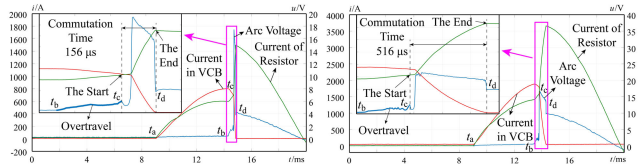

(a) The peak of i_s is 1.5 kA (b) The peak of i_s is 3.5 kA

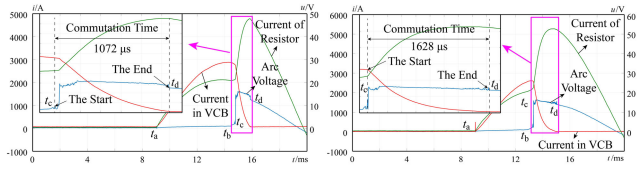

(c) The peak of i_s is 5 kA (d) The peak of i_s is 6 kA

FIGURE 4. The current commutation of 4 mΩ resistor.

drive current of each actuator crosses zero, the corresponding thyristor will naturally cut off. The length of energizing time is related to the parameters of each actuator. In order to better control the sequence of operations, the three actuators in this section are the same model.

A. EXTERNAL FACTORS OF CURRENT COMMUTATION

The external factors that affect the commutation speed include the types of the commutated branches, reactance value, initial phase and current amplitude of the main loop. When the commutated branch is a resistor and the resistance is low (4 mΩ), the change of the commutation time with the current amplitude is shown in Fig. 4 (initial phase: 90°, equivalent inductance of commutated branch $L = 1.2\ \mu$H).

It can be seen that S_2 is closed and the current source is input at t_a. The VCB S_3 is shunted in parallel with the resistor. The actuator of S_3 starts to move at t_b. The overtravel is released during t_b to t_c. The contact pressure decreases and the contact resistance increases, causing the voltage to rise by 1 V-2 V. The contacts are separated at t_c. The arc begins to burn and the voltage rises rapidly, which marks the beginning of the current commutation. Due to the equivalent inductance, the current of commutated branch cannot completely follow the change of the arc voltage, but rises at a different rate until the commutation is completed at t_d. The arc is extinguished and the voltage drops sharply, which marks the end of the commutation. When the peak of i_s is 1.5 kA, the commutation time is 156 μs. The peak current is increased to 3.5 kA, and the commutation time is increased to 516 μs. For the commutated branch of 4 mΩ resistor, when the peak

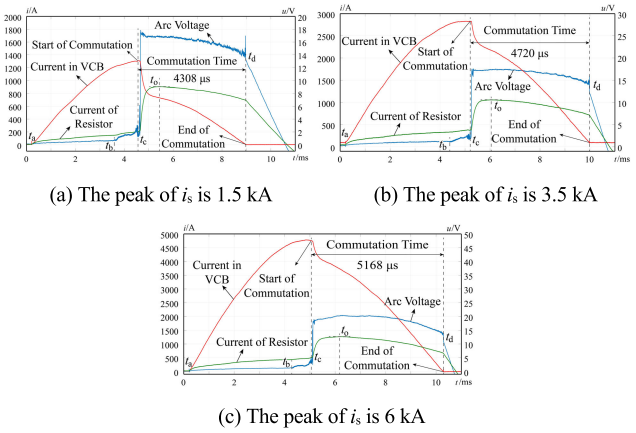

(a) The peak of i_s is 1.5 kA (b) The peak of i_s is 3.5 kA

(c) The peak of i_s is 6 kA

FIGURE 5. The current commutation of 20 mΩ resistor.

current is greater than 5 kA (5 kA, 6 kA), the commutation time is greater than 1 ms (1072 μs, 1628 μs).

The resistance of the commutated branch is increased to 20 mΩ, and the change of the commutation time with the current amplitude is shown in Fig. 5 (initial phase: 90°, $L = 1.2\ \mu$H).

When the peak current is the same, the increase in resistance increases the commutation time. When the contacts are separated at t_c, the arc voltage rises rapidly. The current in the resistor increases rapidly. The current rising rate drops to 0 at t_o, which is clearly different from (a) (b) (c) in Fig. 4. The transient current rising rate (TCRR) of the commutated branch is defined as

$$\frac{di_{pa}}{dt} = \frac{u_{arc} + i_{arc}R_{th2} - i_{pa}R_{th1}}{L} \tag{2}$$

When TCRR is zero, the current of commutated branch cannot continue to increase. If the arc current does not cross zero at this moment, it will be difficult for the AC current commutation to extinguish the arc in a short time. As for the DC commutation, the arc will always be shunted with the commutated branch, resulting in failure of breaking. For a better understanding, let the numerator in (2) be zero, and define the dynamic threshold current as

$$i_{td} = [u_{arc}(t) + i_{arc}(t)R_{th2}]/R_{th1} \tag{3}$$

The dynamic threshold current is time-varying. When i_{pa} reaches the dynamic threshold current, the TCRR is zero. When the resistance is 20 mΩ, it takes about 1 ms from t_c to t_o. After t_o, TCRR is negative. It is difficult for the arc current to cross zero quickly to complete the commutation. When the resistance is 4 mΩ, if the current i_s is low ((a), (b) and (c) in Fig. 4), it is difficult for i_{pa} to touch the dynamic threshold current, so the current commutation is completed quickly within 1 ms. When the peak of i_s increases to 6 kA, i_{pa} just touches i_{td}, and the commutation speed slows down significantly.

The commutated branch is changed to diodes, and the change of the commutation time with the current amplitude is shown in Fig. 6 (initial phase: 90°, $L = 1.2\ \mu$H).

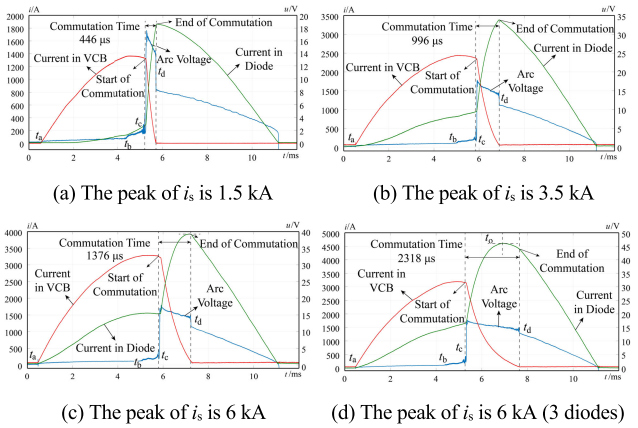

(a) The peak of i_s is 1.5 kA (b) The peak of i_s is 3.5 kA

(c) The peak of i_s is 6 kA (d) The peak of i_s is 6 kA (3 diodes)

FIGURE 6. The current commutation of diodes. The commutated branch is a single diode in (a), (b) and (c). The commutated branch is composed of three diodes connected in series in (d).

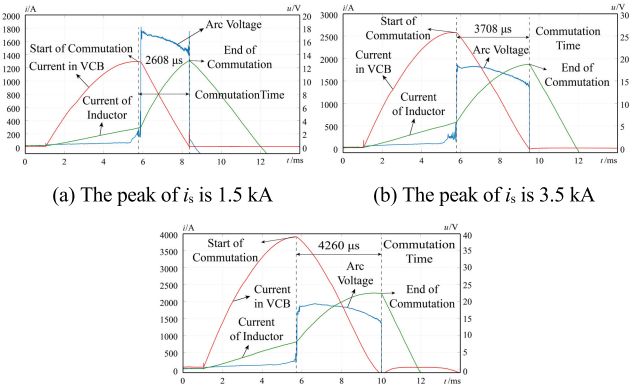

(a) The peak of i_s is 1.5 kA (b) The peak of i_s is 3.5 kA

(c) The peak of i_s is 6 kA

FIGURE 7. The current commutation of an inductor.

When the commutated branch is a single diode, the current commutation is similar to the 4 mΩ resistor. The commutation time increases with the increase of i_s. The TCRR is

$$\frac{di_{pa}}{dt} = \frac{u_{arc} + i_{arc}R_{th2} - u_e - i_{pa}R_{th1}}{L} \tag{4}$$

and the dynamic threshold current is

$$i_{td} = [u_{arc}(t) + i_{arc}(t)R_{th2} - u_e]/R_{th1} \tag{5}$$

When the peak of i_s reaches 6kA, i_{pa} just touches i_{td} at t_o. The number of diodes is increased to 3, and the commutation time is shown in Fig. 6 (d) when i_s is 6 kA. In this case, i_{pa} obviously touches i_{td}, and the commutation time is increased to 2318 μs. Since i_s decreases after t_o, the commutation is barely completed.

The commutated branch is changed to an inductor (25 μH), and the change of the commutation time with the current amplitude is shown in Fig. 7 (initial phase: 90°, equivalent resistance of commutated branch $R_{th1} = 4$ mΩ).

When the commutated branch is an inductor, the TCRR is the same as Eq. (2), but the value of L is much larger. The inductor is made of hollow flat copper wire. TCRR is limited due to the large inductance, which also leads to a long commutation time. Since i_s is a positive AC half wave, it drops in the second half, so the commutation is completed before i_s crosses zero. But the dynamic threshold current is not touched from beginning to end.

It is found through tests that the threshold current is mainly limited by u_{arc}, R_{th1}, R_{th2} and u_e. The TCRR is limited by the value of L. Once i_{pa} touches i_{td}, TCRR will be zero, and the commutated current cannot continue to increase at this time. For DC commutation, the arc will always be shunted with the commutated branch to reach dynamic balance, resulting in failure of breaking. For AC commutation, this will make it difficult to extinguish the arc in a short time. At present, whether in AC or DC applications, most of the commutation branches are power electronics. The equivalent inductance L is very low, so it can be defined as follows. If i_{pa} never touches i_{td} before i_s crosses zero, this commutation is defined as a successful commutation. In order to solve whether the commutation can be successful in practical applications, for any commutation process, when i_{pa} reaches i_{td}, the limit condition is satisfied

$$u_{arc}(t) = [i_s(t)R_{th1} + u_e] - (R_{th1} + R_{th2})\, i_{arc}(t) \tag{6}$$

Simultaneous Eq. (1) and (6), when i_s(t) is known, if $t = t_0$ exists so that (1) and (6) are tenable at the same time, then the commutation process can be judged as failure. The u_{arc} and i_{arc} in the above equations need to be constrained as follows

$$i_{arc}(t) = g_{(x,iarc,mag)}u_{arc}(t) \tag{7}$$

where g is the conductance of the arc. x is the arc length. *mag* represents the influence of the external magnetic field or the magnetic field generated by contacts. In addition, the cathode and anode phenomenon also affects the arc conductance. The literature shows that [16] the arc is diffuse when the arc current is less than 10 kA. The arc above 10 kA may have pinch effect. The peak currents in the experiments in this paper are all less than 10 kA, and the arc is in a diffusion state. Therefore, the anode and cathode phenomenon can be considered to have the same influence on the conductance in each experiment. The conductance g can be obtained by parameters reconstruction in section III.

In practical applications, a lower R_{th2} is often desired. So the feasible way to increase the dynamic threshold current is to increase u_{arc} or decrease R_{th1} and u_e. It makes it harder for i_{pa} to touch i_{td}. TCRR will be increased by reducing L, and the commutation speed will be accelerated.

When the peaks of i_s are 1.5 kA, 3.5 kA and 6 kA, the initial phase is changed from 18° to 162° (1st to 9th ms), and the commutation times are shown in Fig. 8.

Due to the time scatter of the circuit breaker, the initial phase is not exactly the target phase. The relationship between the initial phase and the commutation time can be shown by connecting the results of multiple tests. In summary, when the reactance of the commutated branch is low or the peak of i_s is low, the current is easily commutated. According to previous experience and literature [17], if the total operating time of the circuit breaker is required to be in

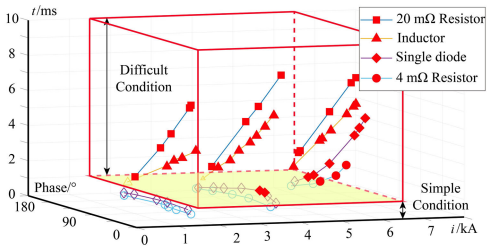

FIGURE 8. **The data points are marked as solid when the commutation time is greater than 1 ms. The data points are marked as hollow when the commutation time is less than 1 ms.**

the millisecond level, no matter in DC or AC applications, the commutation time is not allowed to be too long. If the commutation time can be guaranteed to be less than 1 ms, the requirements of most applications can be met. Therefore, we define the external conditions as simple conditions when the commutation time is less than 1 ms. When the resistance R_{th1}, inductance L, on-state voltage drop u_{e}, i_{s} increases, or the initial phase is changed, the commutation time will increase. The external conditions when the commutation time is greater than 1 ms can be defined as difficult conditions. Under difficult conditions, it is necessary to study the influence of internal factors, so as to explore the acceleration methods of current commutation.

B. INTERNAL FACTORS OF CURRENT COMMUTATION

The controllable internal factors of current commutation include magnetic field and contact velocity. The AMF restrains the arc severely. The radial loss of ions and electrons is reduced. The arc voltage is reduced. According to (5), the dynamic threshold current and TCRR will be reduced. It is not conducive to the acceleration of current commutation. Therefore, the influence of TMF on the commutation process is studied by external permanent magnets in this paper. Two groups of permanent magnets are placed horizontally outside the interrupter at equal distances from the center of the contact. Each group consists of several independent permanent magnets connected in series. The N pole of one group faces the S pole of the other group.

Three difficult conditions are studied, a resistor (20 mΩ, branch 1), three diodes in series (branch 2) and an inductor (25 μH, branch 3). The peak of i_{s} is 6 kA. The transverse magnetic field intensity at the center of two groups of permanent magnets is 25 mT. The commutation processes when the initial phase is about 90° are shown in Fig. 9.

The commutation processes are almost unaffected for branch 1 and branch 3. The commutation time of branch 2 is shortened by only 0.3 ms. Significant acceleration is not found when only the TMF is applied. The permanent magnet actuator (PMA) is used as the opening mechanism in this section. The average opening velocity can be controlled by adjusting the pre-charge voltage of the drive capacitor. The opening displacement and the time scatter of the contacts are shown in Fig. 10 (a) and (b).

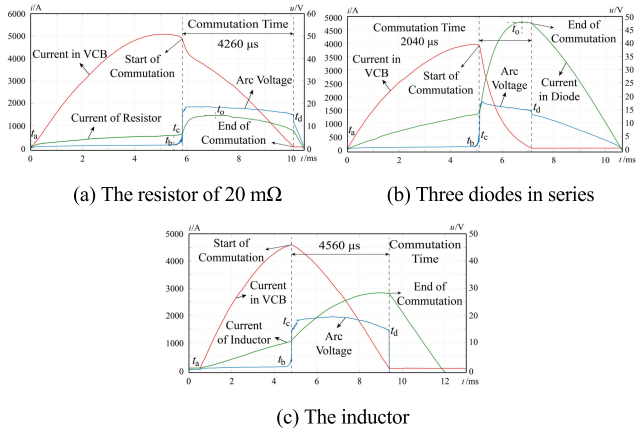

(a) The resistor of 20 mΩ (b) Three diodes in series

(c) The inductor

FIGURE 9. **The effect of applying only TMF on current commutation under difficult conditions.**

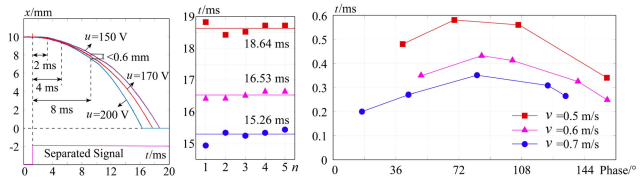

(a) Displacement (b) Time scatter (c) Commutation time of a single diode

FIGURE 10. **The opening characteristics of PMA and its influence.**

The pre-charge voltages are 150 V, 170 V and 200 V. The corresponding average opening times are 18.64 ms, 16.53 ms and 15.26 ms. The average opening velocities are 0.5 m/s, 0.6 m/s and 0.7 m/s. The effect shown in Fig. 10(c) is produced only when the peak current is 1.5 kA and the commutated branch is a single diode. The commutation time is accelerated by a maximum of 0.3 ms. When the conditions are branch 1, branch 2 or branch 3, the commutation time hardly changes. Therefore, the commutation process is not significantly affected by changing the contact velocity in a small range. For difficult conditions, it is difficult to accelerate commutation only by increasing the average opening velocity.

III. PRINCIPLE ANALYSIS OF INTERNAL FACTORS

In order to improve the dynamic threshold current and commutation speed, the interaction theory of TMF and the movement of contact will be studied in this section, so as to obtain an effective acceleration method for current commutation.

A. THE RECONSTRUCTION THEORY OF CASSIE-MAYR PARAMETERS

The effect of internal factors on the arc can be deeply analyzed through the reconstruction of arc parameters. When the arc is in a high current, the mathematical form of the arc can be expressed as the Cassie model

$$\tau_1 \frac{1}{g}\frac{dg}{dt} = \frac{u^2}{E^2} - 1 \tag{8}$$

where τ_1 is the Cassie time constant; E is the Cassie voltage; g is the arc conductance; u is the arc voltage. For any moment

t of the breaking experiment, we take

$$\begin{aligned} \frac{1}{g}\frac{dg}{dt}\bigg|_t &= A_1 \\ \frac{1}{g}\frac{dg}{dt}\bigg|_{t+\Delta t} &= A_2 \\ u^2\big|_t &= B_1 \\ u^2\big|_{t+\Delta t} &= B_2 \end{aligned} \tag{9}$$

Suppose that during Δt, τ_1 and E remain unchanged. Then at time t, Eq. (8) can be written as

$$A_1\tau_1 = \frac{B_1}{E^2} - 1 \tag{10}$$

At $t + \Delta t$, Eq. (8) can be written as

$$A_2\tau_1 = \frac{B_2}{E^2} - 1 \tag{11}$$

Combining (10) and (11), when the breaking experiment is completed, τ_1 and E^2 at any time t can be expressed as

$$\tau_1 = \frac{B_1 - B_2}{A_1B_2 - A_2B_1} \tag{12}$$

$$E^2 = \frac{A_1B_2 - A_2B_1}{A_1 - A_2} \tag{13}$$

Let $\Delta t \to 0$, Cassie parameters at any time in any breaking experiment can be reconstructed as

$$\tau_1 = \frac{d\left(u^2\right)/dt}{u^2 \cdot \frac{d}{dt}\left(\frac{1}{g}\frac{dg}{dt}\right) - \frac{1}{g}\frac{dg}{dt}\left(\frac{d(u^2)}{dt}\right)} \tag{14}$$

$$E = \sqrt{u^2 - \frac{1}{g}\frac{dg}{dt}\frac{d\left(u^2\right)/dt}{\frac{d}{dt}\left(\frac{1}{g}\frac{dg}{dt}\right)}} \tag{15}$$

When the arc is in a low current before zero, the mathematical form of the arc can be expressed as Mayr model. The typical expression is as follows

$$\tau_2\frac{1}{g}\frac{dg}{dt} = \frac{ui}{N} - 1 \tag{16}$$

where τ_2 is the Mayr time constant; i is the arc current; N is the power dissipation of the arc column. In the same way [18], Mayr parameters at any time in any breaking experiment can be reconstructed as

$$\tau_2 = \frac{d\left(ui\right)/dt}{ui \cdot \frac{d}{dt}\left(\frac{1}{g}\frac{dg}{dt}\right) - \frac{1}{g}\frac{dg}{dt}\left(\frac{d(ui)}{dt}\right)} \tag{17}$$

$$N = ui - \frac{1}{g}\frac{dg}{dt} \cdot \frac{d\left(ui\right)/dt}{\frac{d}{dt}\left(\frac{1}{g}\frac{dg}{dt}\right)} \tag{18}$$

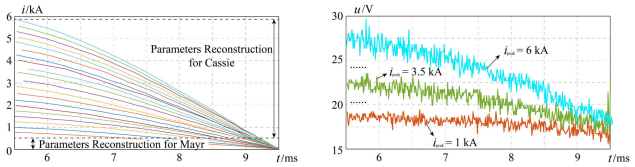

(a) Arc current (b) Arc voltage

FIGURE 11. The breaking experiments without TMF.

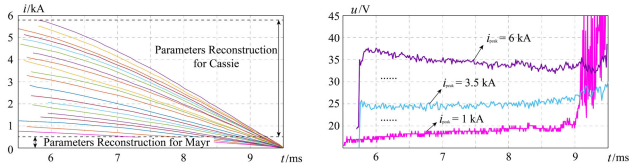

(a) Arc current (b) Arc voltage

FIGURE 12. The breaking experiments with TMF.

B. INTERACTION THEORY OF INTERNAL FACTORS

In order to increase the contact velocity, the opening mechanism is changed to a repulsion actuator. The breaking experiments of the vacuum interrupter are carried out separately with or without TMF. The arc model in both cases are constructed to analyze the interaction theory of TMF and the movement of contact.

The commutated branch T of the experimental topology in Fig. 2 is removed. The capacitor voltage of the current source is adjusted so that the peak value of i_s changes from 1 kA to 6 kA. The step size is 250 A. The total number of arc breaking experiments with and without TMF is 42 times. The current and voltage of breaking are shown in Fig. 11 and Fig. 12.

In the breaking experiments without TMF, the arc voltage increases with the increase of arc current, which reflects the positive resistance characteristics. Comparing Fig. 11(b) and Fig. 12(b), the corresponding voltage under the same current is significantly elevated in the breaking experiments with TMF. When the current is high, the arc voltage decreases as the current decreases. When the current drops, the arc voltage tends to increase obviously. When the peak current is 1kA and the initial phase is about 30°, the arc voltage even keeps increasing. During the low current period before zero, the voltage rises rapidly and the amplitude of the noise increases. This is mainly due to the combined effect of TMF and the rapid increase of the opening distance. Fig. 13 and Fig. 14 shows the Cassie parameters reconstructed from the breaking experiments according to (14) and (15) when the arc current is high.

The threshold current here refers to the current boundary between Cassie and Mayr. Before the current drops to the threshold current, the Cassie parameters can be calculated. After the current is less than the threshold current, the Mayr parameters can be calculated. Connect the corresponding E^2 points when the current is equal to the threshold current to form the C-M boundary. In other words, the C-M boundary is the boundary of the Cassie and Mayr parameters when the

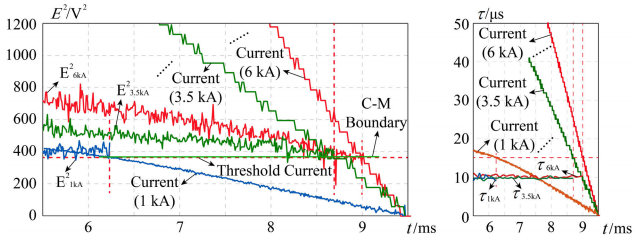

FIGURE 13. E^2 and τ_1 of Cassie model without TMF.

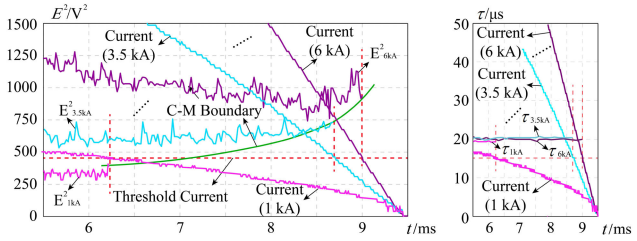

FIGURE 14. E^2 and τ_1 of Cassie model with TMF.

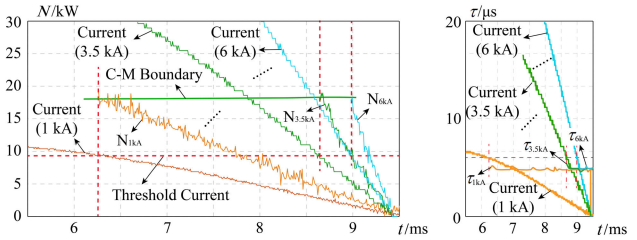

FIGURE 15. N and τ_2 of Mayr model without TMF.

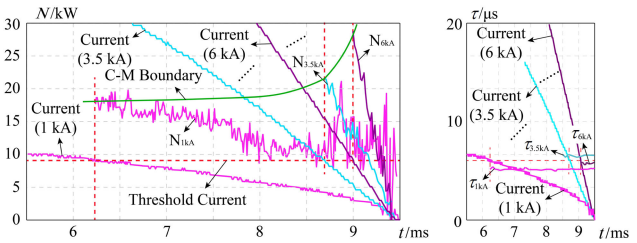

FIGURE 16. N and τ_2 of Mayr model with TMF.

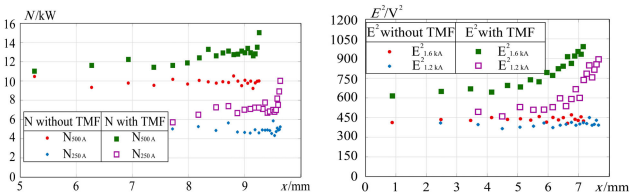

(a) N-opening distance x (b) E^2- opening distance x

FIGURE 17. The decoupling of opening distance-current-TMF.

current is the threshold current. The characteristics of the arc will be affected by TMF from arc shape, plasma evolution, cathode and anode phenomena. This affects the parameters of Cassie and Mayr. The original representation of the Cassie model is

$$\frac{1}{g}\frac{dg}{dt} = \frac{1}{g \cdot P_{loss}^{-1}\left(\frac{dq}{dg}\right)}\left(\frac{g \cdot u^2}{P_{\text{loss}}} - 1\right) \tag{19}$$

where P_{loss} is the power loss caused by energy dissipation; q is the energy of arc column. Comparing (8) and (19), we can see

$$\begin{cases} \tau_1 = g \cdot \left(\dfrac{dq}{dg}\right) \cdot P_{loss}^{-1} \\ E^2 = P_{loss}/g \end{cases} \tag{20}$$

When the power loss increases, the Cassie voltage E increases. When the arc voltage u is greater than E, the arc temperature will increase. Thermal dissociation will increase. The arc conductivity g tends to increase. τ_1 means the time required for the arc resistance to increase n times when the arc current disappears. It can be seen from the figure that E^2 is not a constant, but changes with factors such as current and contacts gap. Compared with the condition without TMF, E^2 in each experimental curve is improved after TMF is applied. This makes it more difficult for the arc voltage u to be greater than E. Thermal dissociation is harder to increase. The conductance g drops. The power loss increases. Due to data noise,τ_1 without TMF is mainly distributed between 5 μs -20 μs. After TMF is applied, τ_1 increases slightly, and the distribution becomes 10 μs- 30 μs. In order to make it clear, the high frequency components in the figure are filtered out. The thermal inertia of the arc increases slightly. Fig. 15 and Fig. 16 shows the Mayr parameters reconstructed from the breaking experiments when the arc current is low.

In the Mayr model, when the arc power is greater than the dissipation power N, the arc temperature will increase. Thermal dissociation will increase. The arc conductivity g tends to increase. Due to the thermal inertia (τ_2) of the arc, the increase in arc temperature or conductance g tends to be slow. Comparing Fig. 15 and Fig. 16, the dissipation power N is also time-varying. Compared with the condition without TMF, N in each experimental curve is improved after TMF is applied. This makes it more difficult for the input power ui to be greater than N. Thermal dissociation is harder to increase. The conductance g drops. Due to the low current, τ_2 is mainly distributed between 5 μs-7 μs with or without TMF. TMF has little effect on the thermal inertia in Mayr model.

It is difficult to discuss the influence of internal factors (the contact velocity, the arc current, and TMF) on arc characteristics from the above experimental curves. Because the opening distance and arc current in each curve change with time. The parameters of Cassie and Mayr model are affected by various factors at the same time. In order to realize the decoupling of opening distance-current-TMF, the change of reconstruction parameters with opening distance are shown in Fig. 17 under the same current.

When the arc current is the same, the application of TMF causes the overall increase of N and E^2. This means an increase in the power dissipation of the arc energy. The increase is small when the opening distance is small. As x increases, the effect of TMF increases rapidly. That is, the opening distance amplifies the effect of the magnetic

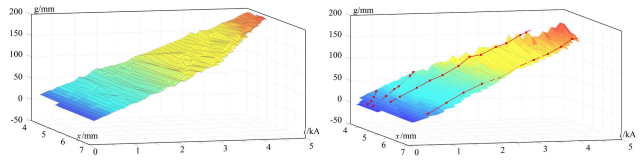

(a) g surface without TMF (b) g surface with TMF

FIGURE 18. The curved surfaces of arc conductance.

field. This also explains why the acceleration effect of TMF is not obvious with PMA in Section II. The PMA only moves 4 mm at the 8th ms. It can be seen from Fig. 17 that this hardly contributes to the increase in power dissipation. In other words, the dissipation power of the arc can be increased faster by applying TMF while increasing the contact velocity. The resistance and voltage of arc will be increased. The current commutation will be accelerated.

Taking x and arc current as the bottom coordinate, and the arc conductance g as the z coordinate, the curved surfaces of arc conductance with and without TMF are calculated by interpolation algorithm, as shown in Fig. 18. The arc conductance becomes smaller due to TMF. (The effect of the opening distance described in this section is actually the combined effect of integration of TMF on time and opening distance. But the amplifying effect of opening distance on TMF is considered to be more powerful in this paper.)

IV. ACCELERATION METHOD AND PROTOTYPE

A. THEORETICAL CRITERION FOR THE SUCCESS OF COMMUTATION

As mentioned before, if i_{pa} never touches i_{td} before i_s crosses zero, this commutation is defined as a successful commutation. Combining commutation equations in Section II, the reconstruction parameters in Section III and Fig. 17, the criterion for the success of the current commutation can be fully described. For any commutation process, the commutation equations can be expressed as

$$\begin{cases} u_{arc}(t) + i_{arc}(t)R_{th2} = u_e + L\dfrac{di_{pa}}{dt} + i_{pa}(t)R_{th1} \\ i_s(t) = i_{pa}(t) + i_{arc}(t) \\ i_{arc}(t) = g u_{arc}(t) \\ g = [1 - \zeta\,(i)]\, g_m + \zeta\,(i)\, g_c \end{cases} \tag{21}$$

where $\zeta\,(i)$ is a step function, which changes from 0 to 1 at the Cassie-Mayr threshold current. g_m and g_c are the conductance in Mayr and Cassie models, which are determined by

$$\tau_1 \frac{1}{g_c}\frac{dg_c}{dt} = \frac{u^2}{E^2} - 1 \tag{22}$$

$$\tau_2 \frac{1}{g_m}\frac{dg_m}{dt} = \frac{ui}{N} - 1 \tag{23}$$

where τ_1, E, τ_2, and N are obtained from the interpolation surface of the opening distance and arc current according to Fig. 17. The limit condition of current commutation can be rewritten as

$$u_{arc}(t) + (R_{th1} + R_{th2})\, i_{arc}(t) = i_s(t)R_{th1} + u_e \tag{24}$$

For any current commutation process of any topology, simultaneous Eq. (21), (22), (23) and (24), when i_s(t) is known, if $t = t_0$ exists so that the equations are satisfied at the same time, then the commutation process can be judged as failure.

B. ACCELERATING EXPERIMENTS OF PROTOTYPE

The 5SHY 42L6500 type IGCT is used as a commutated branch in the previous research 10 kV natural commutation hybrid DCCB [19]–[21]. The voltage drop of a single IGCT is

$$u_{drop} = u_{sh} + iR_{slope} \tag{25}$$

where u_{sh} is the threshold voltage; R_{slope} is the on-state resistance. The maximum turn-off current of a single IGCT is 3.8 kA. The overvoltage when breaking short-circuit current is 2.5 p.u. If the turn-off current capacity is required to be 6 kA, two IGCTs are required to be connected in parallel and then cascaded to 4 levels [22]. According to the data sheet, the voltage drop would be 14 V.

For some hybrid AC fast ATS, the lines waiting to be cut require rapid commutation. Most of them belong to the Power Contactor (PC) class. Only low current can be transferred. If the commutation speed under high current can be increased, the equipment capacity will be increased. This makes it possible to be upgraded to Circuit Breaker (CB) class. The voltage level and breaking capacity of hybrid switches based on vacuum interrupter-power electronics will also be improved. The voltage drop of the commutated branch of this type of equipment is 13 V-14 V according to (25).

The equivalent accelerating experiments are performed using cascaded diodes (ZP600A). According to the data sheet, the on-state voltage drop of ZP600 at rated current is $V_{FM} < 1.8$V. Since it is a sine half-wave current in the experiments, the transient overload capability of the diode is fully utilized. Therefore, two diodes are connected in parallel and then cascaded to 8 levels. The voltage drop is proved by experiments to be equivalent to the actual voltage drop. It can effectively verify the effect of the acceleration method in practical applications.

The analysis in Section III shows that the commutation can be effectively accelerated by applying TMF while increasing the contact velocity. The average opening velocity of the prototype with an electromagnetic repulsion mechanism is 3 m/s. The transverse magnetic field intensity is adjusted to 65 mT. The peak of i_s is 6 kA to verify the acceleration method. The results of the accelerating experiments in different phases are shown in Fig. 19.

The voltage in Fig.19 (b) increases by 2-4 V before the commutation starts. This is because the over-travel force becomes smaller after replacing the repulsion mechanism, which leads to greater contact resistance between the contacts. As long as the current i_s is not affected, this contact

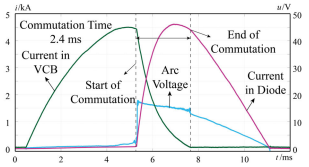

(a) The current commutation before acceleration

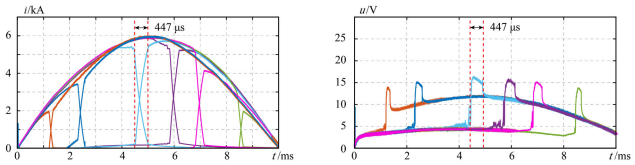

(b) The current commutation after acceleration

FIGURE 19. **The results of the accelerating experiments.**

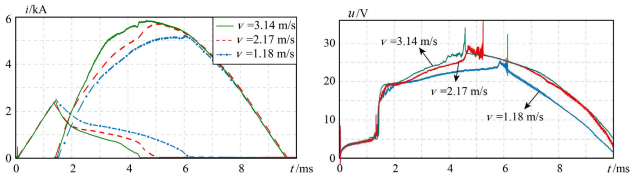

FIGURE 20. **The results at different opening velocities.**

resistance has no effect on the current commutation process after the contacts are separated. After the commutation starts, the arc current decreases rapidly, and the voltage also decreases with the current. Compared with the commutation before acceleration, the commutation time after acceleration is significantly shortened. The commutation time in each phase is less than 0.5 ms. The maximum commutation time is 447 μs. The time requirements of most applications can be met.

The composite switches or high-voltage hybrid phase-control switches often require a lot of power electronic devices [23]–[25]. The voltage drop may reach 20-30 V, which makes natural commutation difficult to complete. The equivalent accelerating experiments of this kind of commutation is also carried out in this section. The results at different opening velocities are shown in Fig. 20.

The fastest average opening velocity is 3.14 m/s, and its commutation time is 1.7 ms shorter than when the velocity is 1.18 m/s. The correctness of the theoretical analysis has been effectively verified. It is proved that the commutation can be effectively accelerated by applying TMF while increasing the contact velocity. If the opening velocity can be further increased, the commutation time will be shorter.

V. CONCLUSION

The external and internal factors affecting the commutation process based on vacuum arc are deeply analyzed in this paper. The criterion for the success of the current commutation is obtained. The internal factors are studied emphatically. The Cassie-Mayr parameters with and without TMF are reconstructed. The decoupling analysis of opening distance-current-TMF is realized. It is concluded that the effect of TMF increases with the increase of opening distance. The acceleration method that increases the opening velocity while applying TMF is proposed. The prototype for accelerating experiments is developed. The following main conclusions can be obtained.

1) The dynamic threshold current is mainly limited by arc voltage u_{arc}, equivalent resistance of the commutated branch R_{th1} and turn-on voltage u_{e}. The TCRR is limited by the reactance of the commutated branch L. For any current commutation process of any topology, the success of current commutation can be judged by whether there is a certain moment t_0, so that the commutation equations, Cassie-Mayr equations, and the limit conditions are satisfied at the same time.

2) The commutation time under difficult conditions is difficult to be shortened by only applying TMF (25 mT) or only changing the opening velocity (0.5 m/s, 0.6 m/s, 0.7 m/s). The reconstruction analysis of Cassie-Mayr parameters shows that the increase of the opening distance obviously amplifies the Cassie voltage E and Mayr dissipation power N. As a result, the arc conductance decreases. The analysis of parameter reconstruction provides theoretical support for similar arc analysis in actual engineering.

3) The average opening velocity of the prototype is 3 m/s. The transverse magnetic field intensity is increased to 65 mT. The peak current of the main loop is 6 kA. When the number of cascaded semiconductor devices is small, the commutation time is shortened from 2.3 ms to 447 μs. The requirements (1 ms) of most applications can be met. When the number is large, the average opening velocity increases from 1.18 m/s to 3.14 m/s, which reduces the commutation time by 1.7 ms. It is proved that the commutation can be effectively accelerated by applying TMF while increasing the contact velocity.

REFERENCES

[1] W. Wen, Y. Huang, Y. Sun, J. Wu, M. Al-Dweikat, and W. Liu, "Research on current commutation measures for hybrid DC circuit breakers," *IEEE Trans. Power Del.*, vol. 31, no. 4, pp. 1456–1463, Aug. 2016.

[2] L. Chen, H. Pan, C. Deng, F. Zheng, Z. Li, and F. Guo, "Study on the application of a Flux-Coupling-Type superconducting fault current limiter for decreasing HVdc commutation failure," *Can. J. Electr. Comput. Eng.*, vol. 38, no. 1, pp. 10–19, Winter 2015.

[3] S. Teng, Z. Zhang, and L. Xiao, "Research on a novel DC circuit breaker based on artificial current zero-crossing," *IEEE Access*, vol. 8, pp. 36070–36079, 2020.

[4] H. Xie and R. Li, "A novel switched-capacitor converter with high voltage gain," *IEEE Access*, vol. 7, pp. 107831–107844, 2019.

[5] B. R. Shrestha, U. Tamrakar, T. M. Hansen, B. P. Bhattarai, S. James, and R. Tonkoski, "Efficiency and reliability analyses of AC and 380 V DC distribution in data centers," *IEEE Access*, vol. 6, pp. 63305–63315, 2018.

[6] J. M. Meyer, H. Duffour, and S. Martin, "An electrical coil module, an electrical coil comprising such modules, an actuation mechanism including such a coil and a circuit breaker comprising such an actuation mechanism," Patent WO 2000 054 292, Sep. 14, 2000.

[7] B. Tian, C. Mao, J. Lu, D. Wang, Y. He, Y. Duan, and J. Qiu, "400 V/1000 kVA hybrid automatic transfer switch," *IEEE Trans. Ind. Electron.*, vol. 60, no. 12, pp. 5422–5435, Dec. 2013.

[8] G. Lv, R. Zeng, Y. L. Huang, and Z. Y. Chen, "Researches on commutating characteristics of mechanical vacuum switch in 10 kV natural-commutate hybrid DC circuit breaker," *Proc. CSEE*, vol. 37, no. 4, pp. 1012–1021, Feb. 2017.

[9] M. Chen, K. Nakayama, S. Zen, and K. Yasuoka, "Threshold current of arc-less current commutation in a hybrid DC switch," *IEEE Trans. Compon., Package., Manuf. Technol.*, vol. 9, no. 6, pp. 1029–1037, Jun. 2019.
[10] S. Wang, L. Y. Zhang, G. H. Yu, and E. Y. Dong, "Hybrid phase-controlled circuit breaker with switch system used in the railway auto-passing neutral section with an electric load," *CSEE J. Power Energy Syst.*, vol. 5, no. 4, pp. 545–552, Dec. 2019.
[11] B. Roodenburg, A. Taffone, E. Gilardi, S. M. Tenconi, B. H. Evenblij, and M. A. M. Kaanders, "Combined ZVS–ZCS topology for high-current direct current hybrid switches: Design aspects and first measurements," *IET Electr. Power Appl.*, vol. 1, no. 2, pp. 183–192, 2007.
[12] Y. Jiang, Y. Liu, Q. Li, J. Wu, J. Cui, and W. Zhang, "External excitation of axial magnetic field for intermediate-frequency vacuum arc research," *IEEE Access*, vol. 7, pp. 161088–161093, 2019.
[13] R. Piovan, L. Zanotto, and T. Bonicelli, "Vacuum breaker for high DC current: Experimental performances and operational limits," *IEEE Trans. Plasma Sci.*, vol. 37, no. 1, pp. 229–235, Jan. 2009.
[14] J. Yuan, J. W. Wu, and J. Bowen, "Reignition after interruption of intermediate-frequency vacuum arc in aircraft power system," *IEEE Access*, vol. 6, pp. 63305–63315, 2018.
[15] H. Chen, X. Liu, L. Li, Y. Liu, Y. Zhang, and Y. Huang, "Analysis of dynamic arc parameters for vacuum circuit breaker under short-circuit current breaking," *IEEE Trans. Appl. Supercond.*, vol. 29, no. 2, pp. 1–5, Mar. 2019.
[16] Z. Liu, S. Xiu, X. Wang, B. Yuan, and R. Li, "The characteristics of vacuum arc in the process of transition to diffuse mode under transverse magnetic field," *IEEE Trans. Plasma Sci.*, vol. 47, no. 8, pp. 3554–3562, Aug. 2019.
[17] T. Zhu, Z. Q. Yu, R. Zeng, G. Lv, Z. Y. Chen, and X. Y. Zhang, "Transient model and operation characteristics researches of hybrid DC circuit breaker," *Proc. CSEE*, vol. 36, no. 1, pp. 18–30, Jan. 2016.
[18] O. E. Gouda, D. K. Ibrahim, and A. Soliman, "Parameters affecting the arcing time of HVDC circuit breakers using black box arc model," *IET Gener., Transmiss. Distrib.*, vol. 13, no. 4, pp. 461–467, Feb. 2019.
[19] W. Wen, Y. Huang, B. Li, Y. Wang, and T. Cheng, "Technical assessment of hybrid DCCB with improved current commutation drive circuit," *IEEE Trans. Ind. Appl.*, vol. 54, no. 5, pp. 5456–5464, Sep. 2018.
[20] S. Shirmohammadi and Y. Suh, "Multiwinding flyback clamp snubber for 10 kV IGCT with reduced voltage stress on clamp recovery diodes," *IEEE Trans. Ind. Appl.*, vol. 56, no. 3, pp. 2729–2740, May 2020.
[21] X. Zhang, Z. Yu, B. Zhao, Z. Chen, G. Lv, Y. Huang, and R. Zeng, "A novel mixture solid-state switch based on IGCT with high capacity and IGBT with high turn-off ability for hybrid DC breakers," *IEEE Trans. Ind. Electron.*, vol. 67, no. 6, pp. 4485–4495, Jun. 2020.
[22] A. Elserougi, I. Abdelsalam, A. Massoud, and S. Ahmed, "Hybrid modular multilevel converter with arm-interchange concept for Zero-/Low-frequency operation of AC drives," *IEEE Access*, vol. 8, pp. 14756–14766, 2020.
[23] O.-B. Hyun, J. Sim, H.-R. Kim, K.-B. Park, S.-W. Yim, and I.-S. Oh, "Reliability enhancement of the fast switch in a hybrid superconducting fault current limiter by using power electronic switches," *IEEE Trans. Appl. Supercond.*, vol. 19, no. 3, pp. 1843–1846, Jun. 2009.
[24] J. Mei, G. Fan, R. Ge, B. Wang, P. Zhu, and L. Yan, "Research on coordination and optimal configuration of current limiting devices in HVDC grids," *IEEE Access*, vol. 7, pp. 106727–106739, 2019.
[25] W. Saito and S.-I. Nishizawa, "Alternated trench-gate IGBT for low loss and suppressing negative gate capacitance," *IEEE Trans. Electron Devices*, vol. 67, no. 8, pp. 3285–3290, Aug. 2020.

LIYAN ZHANG (Graduate Student Member, IEEE) received the B.S. degree in electrical engineering and its automation from Dalian Maritime University, Dalian, China, in 2016. He is currently pursuing the Ph.D. degree in electric machines and electric apparatus with the Dalian University of Technology. His research interests include hybrid circuit breakers, current commutation, controlled switches, and magnetic field control of vacuum arc.

ENYUAN DONG (Member, IEEE) received the M.S. degree in electric machines and electric apparatus from the Shenyang University of Technology, in 1998, and the Ph.D. degree in mechanical electronic engineering from the Dalian University of Technology, in 2004. He is currently a Professor with the Dalian University of Technology. His research interests include speed control of vacuum circuit breakers, hybrid DC circuit breaker, and permanent magnet linear synchronous motor characteristics.

RUIDA ZHUANG received the B.S. degree in thermal energy and power engineering from Jimei University, Xiamen, China, in 2006, and the M.S. degree in electrical engineering from the Dalian University of Technology, Dalian, China, in 2013. His research interests include smart grid and flexible power supply.

YONGXING WANG (Member, IEEE) was born in 1973. He received the B.S. degree from the Hebei University of Technology, Tianjin, China, in 1993, the M.S. degree in electrical engineering from the Huazhong University of Science and Technology, Wuhan, China, in 1996, and the Ph.D. degree in electrical engineering from the Darmstadt University of Germany, Darmstadt, Germany, in 2005. His current research interests include intelligent detection of arc faults, cable insulation testing and state assessment, and aviation electrical system simulation.

YU ZHU (Graduate Student Member, IEEE) received the B.S. degree in electrical engineering and automation from the Dalian University of Technology, Dalian, China, in 2015, where he is currently pursuing the Ph.D. degree in electric machines and electric apparatus. His research interests include arc extinguishing, fault current limiter, and dc circuit breaker-based on current commutation.

JIYAN ZOU received the B.S. degree from Shenyang Industrial University, Shenyang, China, in 1982, the M.S. degree from the Chinese Academy of Sciences electrician, Beijing, in 1984, and the Ph.D. degree in electrical engineering from Xi'an Jiaotong University, Xi'an, in 1987. He is currently a Professor at the Dalian University of Technology. He has numerous publications and patents in many fields, including synchronous switching and high-voltage vacuum circuit breakers. His research interests include intelligent high-voltage electrical apparatus, dc circuit breakers, and pulsed power.